AIP | Applied Physics Letters

A piezoelectric multilayer-stacked hybrid actuation/transduction system

Tian-Bing Xu, Xiaoning Jiang, and Ji Su

Citation: Appl. Phys. Lett. **98**, 243503 (2011); doi: 10.1063/1.3600057
View online: http://dx.doi.org/10.1063/1.3600057
View Table of Contents: http://apl.aip.org/resource/1/APPLAB/v98/i24
Published by the American Institute of Physics.

A piezoelectric multilayer-stacked hybrid actuation/transduction system

Tian-Bing Xu,[1,a)] Xiaoning Jiang,[2] and Ji Su[3]
[1]*National Institute of Aerospace, 100 Exploration Way, Hampton, Virginia 23666, USA*
[2]*Department of Mechanical and Aerospace Engineering, North Carolina State University, Raleigh, North Carolina 27695, USA*
[3]*NASA Langley Research Center, Hampton, Virginia 23681, USA*

(Received 26 April 2011; accepted 23 May 2011; published online 13 June 2011)

A piezoelectric multilayer-stacked hybrid actuation/transduction system (stacked-HYBATS) is reported in this letter. It uses synergetic contributions from positive-strain and negative-strain piezoelectric multilayer-stacks to give displacements of about 3.5 times those of the same-sized piezoelectric flextensional actuator/transducer. The resonance of a stacked-HYBATS is enhanced comparing with that of actuators with either stack alone. The effective piezoelectric coefficient of the stacked-HYBATS is 2.5×10^6 pm/V at the resonance frequency and 1.5×10^5 pm/V at off-resonance frequencies. The stacked-HYBATS provides an approach for high performance electromechanical devices. © *2011 American Institute of Physics*. [doi:10.1063/1.3600057]

Many civilian and military applications, such as active vibration control, flow dynamic control of aircraft, underwater detection, position control of instrumentation, and fuel control of combustion for space propulsion systems, require high performance electromechanical actuators. Since metal-piezocomposite actuators were invented, many device configurations have been exploited for amplifying displacement and enhancing efficiency.[1–8] Among them, a hybrid actuation system (HYBAS) showed significantly enhanced electromechanical performance by using two types of electroactive materials in a cooperative and effective way.[6–8] Using piezoelectric multilayer-stacks in a HYBAS should further enhance its mechanical energy output.[9] In this letter, the actuation performance is presented for such a piezoelectric multilayer-stacked hybrid actuation/transduction system (stacked-HYBATS).

The stacked-HYBATS is shown schematically in Fig. 1(a). The central negative-strain component (NSC) is operated in a "31" (or transverse) mode, while the two outside curved positive-strain components (PSCs) are operated in a "33" (or longitudinal) mode. The three components are connected together at their ends via two passive rigid frames. The stacks are constructed using 0.025 mm thick brass shims and thin layers of epoxy between poled piezoelectric ceramic plates with Cr/Au electrodes on two opposing sides. The precurvature of the PSC is designed so that PSC bends outward and the stress can be distributed uniformly under an applied electric field. So that the shape of the PSCs is[8,10]

$$z(x) = \frac{1}{c}\left[\left(\frac{L}{2}\right)^2 - (x)^2\right]^2, \qquad (1)$$

where x is the position along the X direction (Fig. 1), $z(x)$ is the displacement in the Z direction of the PSC at any x referred to the two ends of the PSC as shown in Fig. 1(a), c is a constant, and L is the distance between the two ends of the PSCs in the X direction.

The stiffness of the NSC is designed to be much higher than that of the two PSCs so that the length of a stacked-HYBATS along the X direction can be controlled by the deformation of the NSC and calculated by[8]

$$L = L_0\left(1 + \frac{L_e}{L_0}d_{31}E\right) = L_0\left(1 + \frac{L_{N0}}{L_0}d_{31}E\right), \qquad (2)$$

where L_0 is the original length of a NSC, L_e is the effective length of a NSC (the length of the electroactive portion), d_{31}

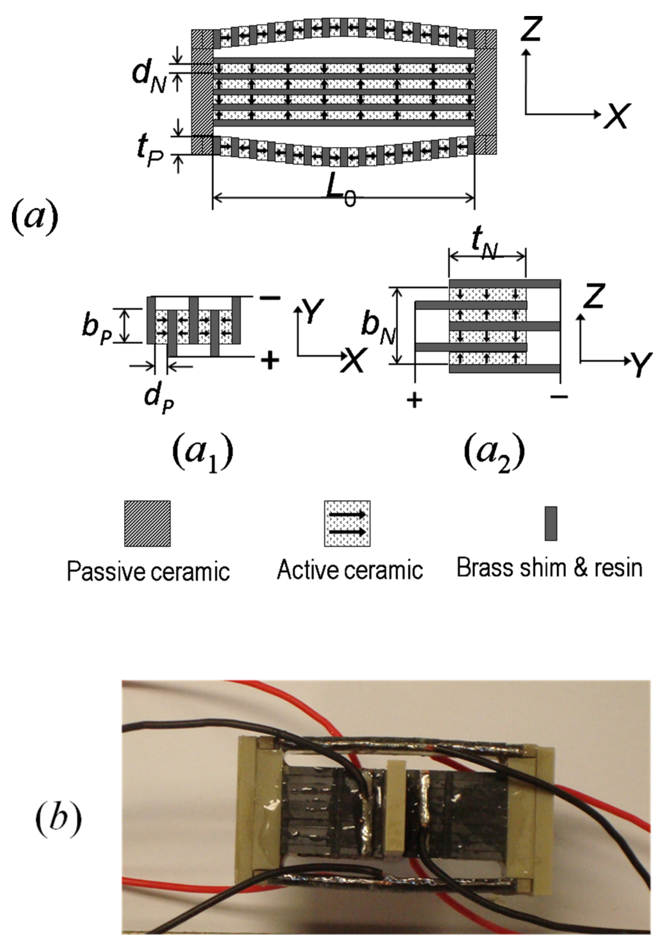

FIG. 1. (Color online) Stacked-HYBATS (a) the diagram for the specific stacked-HYBATS, (a_1) is the top view of a partial PSC, and (a_2) is the cross section view of a NSC; (b) the picture of a prototyped stacked-HYBATS.

[a)]Electronic mail: tbxu@nianet.org.

TABLE I. The parameters of the stacked-HYBATS.

Items		Stacked-HYBATS Symbol	Stacked-HYBATS Value	PSC (one side) Symbol	PSC (one side) Value	NSC Symbol	NSC Value
Length (mm)	Overall	X_0	35.5		31.0		25.0
	Effective	L_0	25.0	L_{P0}	27.5	L_{N0}	23.0
Width (mm)	Overall		10.0		10.0		10.0
	Effective		10.0	b_P	10.0	b_N	10.0
Thickness (mm)	Overall	Z_0	18.0				
	Effective		18.0	t_P	1.0	t_N	10.0
Piezoelectric plate in PSC and NSC	Thickness (mm)			d_P	0.60	d_N	1.0
	Number of layers				43		10

is the transverse piezoelectric coefficient of each piezoelectric plate in a NSC, and E is the applied electric field.

The curvature length of a PSC is integrated by[8]

$$L_{\mathrm{PSC}} = \int_{-L/2}^{L/2} [(dz(x)/dx)^2 + (1)^2]^{1/2} dx. \tag{3}$$

The deformed curvature length L^d_{PSC} of a PSC as a function of the applied electric field is also calculated as

$$L^d_{\mathrm{PSC}} = L^i_{\mathrm{PSC}}\left(1 + \frac{nt}{L^i_{\mathrm{PSC}}} d_{33}E\right), \tag{4}$$

where L^i_{PSC} is the initial length of the PSC, d_{33} is the longitudinal piezoelectric coefficient, t is the thickness for each piezoelectric plate, and n is the number of piezoelectric ceramic layers in each PSC. A 30% length deduction is taken for L^d_{PSC} based on our previous experimental results for piezoelectric 2-2 composite in this scale.

For the experimental study, a device was constructed with the dimensions listed in Table I. The initial condition for the PSCs is set so that the initial center displacement (at $x=0$) $z_i(0)=0.25$ mm, and; the initial c constant was obtained as $c_i=47\,000$ mm^3 from Eq. (1) with the initial length $L_0=25$ mm. TRSHK1 HD piezoelectric ceramic material was used for fabrication of both PSCs and NSC ($d_{33}=750$ pC/N, $d_{31}=-360$ pC/N).[11] Loctite Hysol Epoxy Resin RE2039 was used as the adhesive for the PSCs, NSC, and component integration. A mold following the curve described by Eq. (1) and the initial c_i and L_0 assist in the fabrication of the curved PSCs. An inactive ceramic bar at the center of the NSC was used for the purpose of handling and positioning the stacked-HYBATS during actuation tests.

The mechanical loading capability of the stacked-HYBATS was evaluated at room temperature under a 30 N static force plus 17 N_{rms} dynamic force from 10 kHz down to 0.5 Hz. Displacements were measured using a laser vibrometer (Polytec PI, Inc., model OFV-512) having a laser beam 5 μm in diameter.[7,8] A dc bias voltage slightly higher than the peak value of the ac voltage was applied in order to avoid depoling of piezoelectric components. The frequency spectra were measured at 1 V_{rms}.

Measured displacement profiles of the stacked-HYBATS under the driving of 150 V dc bias and 1 Hz 100 V_{rms} ac for three different actuation modes are shown in Fig. 2. The device was operated under three different modes: (a) only NSC is active, (b) only two PSCs are active, and (c) both NSC and PSCs are active. A stacked-HYBATS with only the NSC active is equivalent to a same-sized flextensional actuator/transducer.[5] The cooperative contraction of the NSC and expansion of the PSCs results in an enhanced motion along the Z direction so that the measured displacement of the stacked-HYBATS is 3.5 times that of the actuation with the NSC alone. Applying voltage only to the PSCs gives a center displacement 2.6 times that of the NSC only. This is due to (1) the higher piezoelectric constant used in the PSCs (d_{33} is about twice d_{31}); (2) the higher electric field in the PSCs (the thickness of each layer in the PSC is 0.6 times that of the NSC); and (3) the higher effective length of the PSCs (1.08 times that of the NSC).

The measured displacements in Z direction at the center as a function of applied voltage for the stacked-HYBATS and also for the NSC in its length direction, as well as the displacement ratio of these two are presented in Fig. 3. The displacements of the NSC predicted theoretically with Eq. (2) are also presented, and they matched well with the measured results.

Given an applied voltage, the L is calculated by the Eq. (2), and L^d_{PSC} by the Eq. (4), separately. Substituting Eq. (1) into Eq. (3), it can be rewritten as

$$\int_{-L/2}^{L/2} \sqrt{1/c^2(4x^3 - L^2x)^2 + 1} \cdot dx = L^d_{\mathrm{PSC}}. \tag{5}$$

The constant c can be calculated for given L and L_{PSC} from Eq. (5) with the finite element method. The displacement profile $z(x)$ can be obtained from Eq. (1) for various c values.

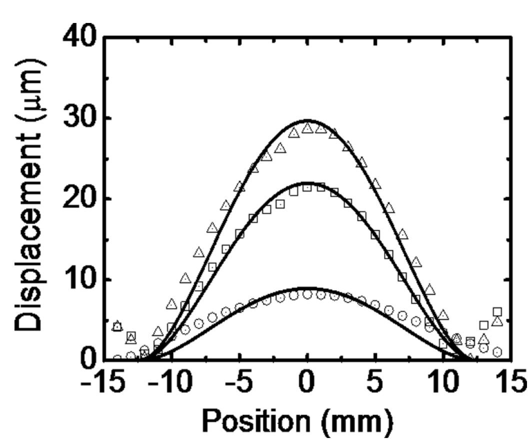

FIG. 2. Displacement profiles of stacked-HYBATS with different working modes at 150 V dc bias and 1 Hz 100 V_{rms}. The symbols represent that the voltage applied to the PSCs only (□), the NSC only (○), and the PSCs and NSCs simultaneously (△). The three solid lines from bottom to top are modeling results divided by 5 for NSCs, PSCs, and stacked-HYBATS, respectively.

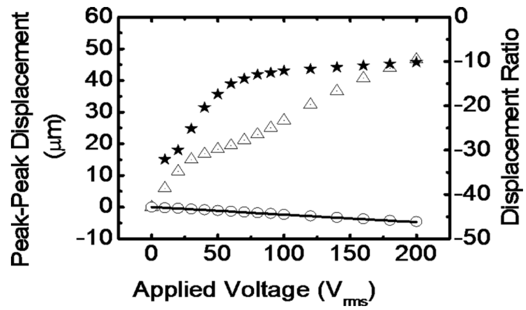

FIG. 3. Displacements and displacement ratio as function of applied voltage for the stacked-HYBATS. They are measured center displacements in Z direction for the stacked-HYBATS (△), measured (○) and modeled (solid line) displacements for the NSC in its length direction in the stacked-HYBATS, and the displacements ratio (★) for the two situations.

The displacement profiles for stacked-HYBATS, i.e., $z_{\text{stacked-HYBATS}}(x)=2[z(x)-z_i(x)]$ can be further calculated.

As shown in Fig. 2, the measured displacements are significantly smaller than the modeling predictions. This may be due to (1) the imperfection of PSCs: the effective length of the PSC was longer than the length of the stacked-HYBATS and the shape of the precurvatures was imperfect, as shown in Fig. 1(b); (2) the deformation absorption by the bonding resin in the PSCs is higher than the prediction of 30% because of the compression stress from the two ends in the stacked-HYBATS; (3) the gaps between NSC and two PSCs are too big; (4) the stiffness of the adhesive resin at the two ends of the stacked-HYBATS may not be high enough to hold the components without relative motion between the passive and active components, which can be confirmed by the unexpected extra displacements observed at the two ends; (5) the thickness of the PSCs is too big comparing with its length to be ignored for the modeling; and (6) the meshing limitation of the ORINGIN software for calculation of the c constant. Therefore, the performance of a stacked-HYBATS can be further improved by design using advanced software and assembly optimizations.

The frequency spectra of displacements for the stacked-HYBATS in three different working modes at 1 V_{rms} is shown in Fig. 4. All the elements have strong resonance peaks. The displacements at frequencies below 1 kHz remain constant. A strong resonance peak, in which the displacement is 15 times the displacement at off-resonance frequencies, is observed at the frequency of 4830 Hz for the stacked-HYBATS in Fig. 4. The details of resonance peaks are observed and presented in the inset in Fig. 4(a). One significant resonance peak for the PSCs-active-only mode is located at 4850 Hz. However, two significant resonance peaks at 4850 and 5300 Hz are observed for the NSC active only as well as for the stacked-HYBATS. The ratio of the two resonance frequencies is 1.093. This may be due to (1) the mismatch between the effective lengths of the PSCs (27.5 mm) and the length of the stacked-HYBATS (25 mm) shown in Fig. 1(b), (2) the precurvature of the PSCs, and (3) the different thicknesses between the PSCs and the NSC.[12] Therefore, the two peaks for the stacked-HYBATS could be pulled together forming an enhanced resonance peak by optimizing the dimensions of the PSCs and the NSC. From Fig. 4 the effective piezoelectric coefficient (EPC) of the stacked-HYBATS can be calculated using the displacement divided by the applied voltage. The obtained EPC for the stacked-HYBATS is 1.5×10^5 pm/V (≅pC/N), which is one order of magnitude higher than the Cymbal[5] at off-resonance frequencies, and 2.55×10^6 pm/V at the resonance frequency. The EPC can be further increased by reducing the thickness of each piezoelectric layer in the PSCs and the NSC, replacing the TRSHK1 HD with higher piezoelectric coefficient materials, or reducing the degree of the precurvature of the PSCs.

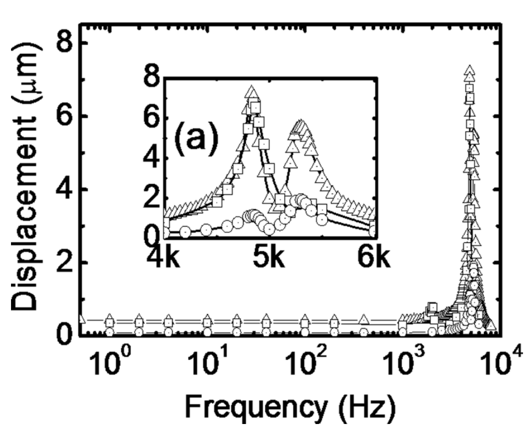

FIG. 4. Frequency spectra of displacements with different working modes for the stacked-HYBATS at 1 V_{mrs}. Symbols are experimental results for stacked-HYBATS (△), PSCs actuation only (□), and the NSC actuation only (○). The inset (a) is the resonance peaks for the three actuation modes (the same definitions for titles and units of axes as well as symbols in the inset of the figure).

In summary, a stacked-HYBATS concept utilizing cooperative contributions of the electromechanical responses of multilayer stacked PSCs and NSC to give significantly enhanced electromechanical performance was demonstrated. The displacement of the stacked-HYBATS is 3.5 times higher than the NSC actuation only, which would be equivalent to a same-sized flextensional actuator. The coupled resonance of a stacked-HYBATS is much stronger than the resonance of an actuation with either PSC or NSC active only. The stacked-HYBATS features high mechanical load capability (no damage with 17 N_{rms}, i.e., 48 N peak-to-peak dynamic force) and low driving voltage compared with our previously reported HYBAS,[7] as well as high EPC and large displacements compared with same-sized conventional piezoelectric actuators.

[1]K. Uchino, *Ferroelectric Devices* (Marcel Dekker, New York, NY, 2000).
[2]R. E. Newnham, Q. C. Xu, and S. Yoshikawa, U.S. Patent No. 4,999,819 (1991).
[3]Z.-Y. Cheng, T.-B. Xu, Q. M. Zhang, R. J. Meyer, D. V. Tol, and J. Hughes, IEEE Trans. Ultrason. Ferroelectr. Freq. Control **49**, 1312 (2002).
[4]R. F. Hellbaum, R. G. Bryant, and R. L. Fox, U.S. Patent No. 5,632,841 (1997).
[5]A. Dogan, K. Uchino, and R. E. Newnham, IEEE Trans. Ultrason. Ferroelectr. Freq. Control **44**, 597 (1997).
[6]J. Su and T.-B. Xu, U.S. Patent No. 7,394,181 B2 (2008).
[7]J. Su, T. Xu, S. Zhang, T. Short, and Q. M. Zhang, Appl. Phys. Lett. **85**, 1045 (2004).
[8]T.-B. Xu and J. Su, J. Appl. Phys. **97**, 034908 (2005).
[9]T.-B. Xu, X. Jiang, and J. Su, U.S. Patent Publication No. 20100096949 (2010).
[10]R. A. Walsh, *Electromechanical Design Handbook* (McGraw-Hill, New York, 2000), p. 5.34.
[11]TRS Technologies Inc., www.trstechnologies.com.
[12]R. D. Blevins, *Formulas for Natural Frequency and Mode Shape* (Krieger, Florida, 1995).